Multimodal Imaging of a Mouse Model of Colorectal Carcinoma Metastasis in the Liver

Rajiv Ramasawmy[1,2], Sean Peter Johnson[1,2], Thomas Anthony Roberts[1], Daniel J Stuckey[1], Anna L David[3], Rosamund Barbara Pedley[2], Mark Francis Lythgoe†[1], Bernard Siow†[1], and Simon Walker-Samuel†[1]

[1]*Centre for Advanced Biomedical Imaging, University College London, London, Greater London, United Kingdom,* [2]*Cancer Institute, University College London, London, Greater London, United Kingdom,* [3]*Institute for Women's Health, University College London, London, Greater London, United Kingdom*

TARGET AUDIENCE: This work will interest researchers of pre-clinical models of cancer, multi-modal imaging and hepatic diseases, as well as researchers looking for cost-effective MRI alternatives to high-field scanners.

INTRODUCTION: The recent availability of permanent low-field, "bench-top" MR scanners for small animal imaging offer potential cost-saving over higher field alternatives due to reduced running and infrastructure expenses. The basic imaging offered by these machines allows for non-specialised applications such as the measurement of the growth of orthotopic tumour xenograft models in mice or rats. Unlike conventional subcutaneous xenograft models, which are implanted under the skin and their growth typically monitored by palpation and/or caliper measurement, orthotopic models grow in the clinically relevant organ. The siting of tumours in organs such as the brain or liver allows straightforward characterisation with MRI, enabling tumour volumes to be accurately measured and thus therapy start-points in studies can be reliably defined. In this study, the ability of three low-cost imaging techniques (1T MRI, ultrasound and bioluminescence imaging (BLI)) to detect and quantify the growth of tumours in a mouse model of colorectal liver metastasis[2] is assessed and compared to 9.4T MRI.

METHODS: Animal model: The SW1222 colorectal carcinoma cell line was injected intrasplenically at a concentration of $1x10^6$ cells in 100 µl in serum free media into 8 MF1 *nu/nu* mice. Cells were allowed to wash through to the liver for 1 minute followed by splenectomy. All mice were imaged on all modalities once a week for 4 weeks following surgery.

BLI (Photon Imager Optima, Biospace Lab, France): Animals were imaged at 15 minutes post intraperitoneal (150 mg/kg) injection of D-luciferin (Biosynth, USA), exposure time 10 seconds. Photon count was calculated as photon emitted per second per steradian (p/s/str) using M3 Vision software (Biospace Lab).

9.4T MRI (VNMRS, Agilent Technologies, CA, USA). *High Resolution Anatomical:* Respiratory-triggered, axial multi-slice fast spin echo, 192^2 matrix, FOV 30 mm^2, slice thickness 0.75 mm, (30 slices to cover the liver), ETL 4, effective TE 19 ms, TR 2s, 3 averages, acquisition time 9 minutes. Sequence parameters were optimised using our previous measurements of liver and tumour T_1 and T_2 at 9.4T.

1T MRI (ICON, Bruker BioSciences Corporation, Ettlingen, Germany). *High Resolution Anatomical:* Respiratory-triggered, axial multi-slice fast spin echo, 192^2 matrix, FOV 30 mm^2 (in-plane resolution 0.156 x 0.156 mm^2), slice thickness 0.75 mm, ETL 12, effective TE 32 ms, TR 2.8s, 3 averages, acquisition time 26 minutes. Sequence parameters were optimised using our previous measurements of liver and tumour T_1 and T_2 at 1T[3].

US (Vevo 2100 system, VisualSonics, Canada) 3D sagittal acquisition with a stepping motor and an MS550D transducer (resolution 0.018 x 0.018 x 0.076 mm^3), imaging time 1 minute.

Image Analysis: Liver and tumour volumes were estimated by manual segmentation of the 1T and 9.4T MRI. Tumour burden was estimated from the ratio of tumour to liver volume. For US data, 3 sets of 10 representative, contiguous slices were analysed per liver volume to match the number of slices in the MRI analysis. Data was blindly assessed by two experienced pre-clinical scientists of each modality. 3D anatomical representations were generated using Amira 5.4 (Visage Imaging, USA). Doubling time was calculated by fitting an exponential function to each animal's tumour burden with time. The coefficients of variability was calculated for inter- and intra-user variability (CoV = 100% * std/mean) from five duplicate datasets. CNR (tumour *vs* liver) was calculated from mice in week 4 post implantation, using the following equation: $CNR = (S_{Liver} - S_{Tumour})/\sqrt{\sigma_{Liver}{}^2 + \sigma_{Tumour}{}^2}$.

RESULTS: In both 1T and 9.4T, T_2-weighted images (Fig 1A) the tumour regions appear hyper-intense (arrow) relative to the liver tissue (red outline). In the US images, the tumour regions appear hypo-intense (arrow) relative to the liver signal (red outline). US images also displayed regions of signal loss (star) due to rib shadowing. Visual comparison of 3D volumes (Fig 1B) over weeks 2-4 in an example mouse shows similar localised development of the tumours (yellow) in the whole liver (red). Mean tumour burden growth rates (Fig 1C) showed no significant difference (ANOVA, $p > 0.05$) between doubling times (mean ± std): 2.9 ± 1.1 days (9.4T MRI), 1.8 ± 0.6 days (1T MRI), and 3.0 ± 1.5 days (US). The mean log BLI flux over the four weeks (Fig 1E), from a ROI over the liver, shows a large increase and eventual plateau, contrary to the other three modalities. A comparison of a day-matched 9.4T MRI tumour burden and BLI flux (Fig 1F) shows a strong correlation ($p < 0.01$). Finally, CNR (liver vs tumour) was 4.9 ± 1.4 (9.4T MRI), 2.5 ± 0.9 (1T MRI) and 0.4 ± 0.1 (US), which was reflected in the intra-user CoV (4.7%, 11.1%, 14.3%, respectively), but not the inter-user variability (7.0%, 13.3%, 9.9%, respectively).

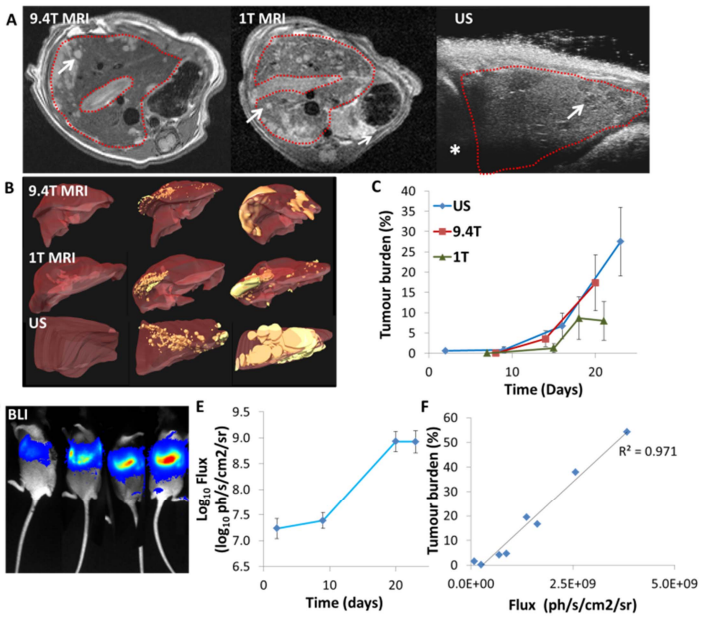

Figure 1: (A) 9.4T, 1T and US images of liver (red outline) and metastases (arrow). (B) 3D representations of liver (red) and tumour (yellow) volumes after manual segmentation of an example data set from weeks 2-4. (C) Tumour growth curves of liver tumour burden, based on image segmentation. (D) BLI images from weeks 1-4 (left to right) from an example mouse. (E) Mean BLI log flux against time. The flux increases until day 20 when the signal plateaus due to signal saturation. (F) BLI flux from mouse livers showed a significant correlation with gold-standard 9.4T MRI estimation of tumour burden at day 20 ($p < 0.01$).

DISCUSSION: This study compared three relatively low-cost and compact imaging methods for measuring tumour burden in an orthotopic mouse model of colorectal liver metastasis. Ultrasound and 1T MRI agreed well with gold-standard 9.4T measurements. Variability of user-determined tumour burden was comparable between 1T and US, reflecting the trade-off between high resolution and contrast to noise offered by each. 9.4T MRI had the greatest contrast between tumour and liver, as expected, however the 1T MRI and US may be potentially improved with contrast agents. 1T MRI is able to provide quantitative data not only of tumour burden but also total tumour volume across the whole liver. Although the sensitivity is not as good as 9.4T it has a higher CNR when compared to US. Ultrasound imaging provides a fast, high resolution method of imaging, although CNR was very low. For this analysis a tumour burden value was estimated from a partial liver segmentation, however, despite assuming a homogenous distribution across the liver, the estimated tumour burden agreed well with the 9.4T MRI. Bioluminescence imaging offered a semi-quantitative measure of tumour burden via photon flux signal, and though the growth curves do not follow exponential growth, the measured flux corresponded well with the 9.4T estimate of tumour burden. The high sensitivity of BLI makes it a useful tool for high-throughput screening of cell engraftment, though the accurate measurement of tumour volume, even using multiple orientations will be semi-quantitative. The imaging modality used should therefore be dependent on the expected endpoint of the biological parameter to be assessed, however as a low cost, easy to use modality that offers the best alternative to 9.4T for routine and varied use, imaging with 1T MRI and high-resolution ultrasound offer promise for low-cost, accurate measurement of tumour burden in orthotopic tumour xenograft models.

REFERENCES: [1] A. Schmid et al. *Mol. Imaging Biol.* (2013), **15**:155-165. [2] Dearling,J.L. *et al. Nucl. Med. Biol.* 2009; 36, 883-894. [3] R. Ramasawmy, *et al. Proc. Intl. Soc. Magn Reson Med* (2014), **22**:1153. [4] P. Caravan et al. *Contrast Media Mol. Imaging* (2009), 4:89-100. *†Joint Senior Authors*